

# The effect of oxygen partial pressure on the oxidation behaviour of carbon fibres and carbon fibre/glass matrix composites

R. G. IACocca

*Department of Engineering Science and Mechanics, The Pennsylvania State University, University Park, PA 16802, USA*

D. J. DUQUETTE

*Department of Materials Engineering, Rensselaer Polytechnic Institute, Troy, NY 12180, USA*

Carbon fibres were examined for oxidative stability, both in the as-received condition and in a carbon fibre/glass matrix composite, to determine the effect of oxygen partial pressure on their oxidation behaviour. The oxidation data as a function of oxygen partial pressure (0.05, 0.21, and 1.0 atm) were then analysed to determine how the structure of the fibre surface impacts the oxidation behaviour. For the as-received material, it was determined that the data are best described by Temkin-type adsorption kinetics, while the fibres encased in the glass matrix exhibited Langmuir-type kinetics. This relevance of this distinction is discussed.

## 1. Introduction

Carbon fibres have been identified as a possible reinforcing material for intermediate- and high-temperature composite materials. Before these fibres can be placed in these high-performance materials, however, their oxidative stability must be fully characterized and understood. Previously published data have shown the effects of matrix microcracks on the oxidation behaviour of carbon fibre/glass matrix composites [1], and the effect of a catalyst on the oxidation behaviour and microstructural integrity of carbon fibres [2]. The purpose of this study was to examine the effect of oxygen partial pressure on the oxidation behaviour of the carbon fibres and carbon fibre/glass matrix composite materials to gain a more fundamental understanding into how the structure of the fibres affects their oxidation behaviour.

## 2. Materials characterization

### 2.1. Carbon fibres

All of the ex-PAN (polyacrylonitrile) carbon fibres used in this investigation were supplied by Fortafil Fibers, Inc., on three large spools, with each spool containing a "tape" of fibres. This tape consisted of four fibre tows (50 000 filaments per tow) in width (approximately 100 mm) and 60 m long, and were backed by a strip of paper. Table I shows a list of properties for the as-received fibres.

It has been well documented that many different types of carbon fibres do not exhibit an isotropic structure. Ex-PAN-based fibres are included in this category. Fig. 1 shows a schematic drawing of a typical PAN fibre [3]. The outer skin consists of oriented crystallites of grapheme – a two-dimensional sheet of

TABLE I Nominal properties for Akzo 5C fibres

Tensile strength	$400 \times 10^3$ p.s.i.	2760 MPa
Tensile modulus	$50 \times 10^6$ p.s.i.	345 GPa
Ultimate elongation	0.8%	0.8%
Density	$0.065 \text{ lb in}^{-3}$	$1.8 \text{ g cm}^{-3}$
Filament shape	Round	Round
Filament diameter	$0.28 \times 10^{-3}$ in	7 $\mu\text{m}$

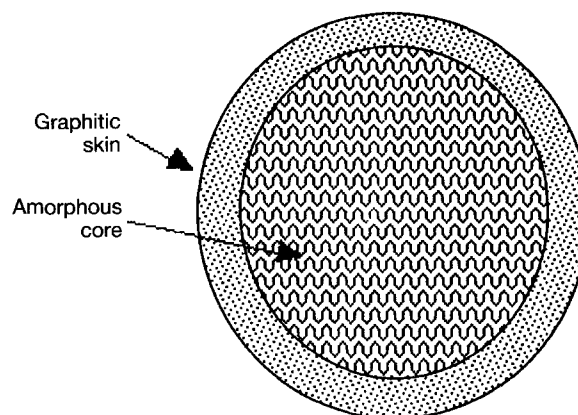


Figure 1 Schematic drawing of ex-PAN-based fibres showing skin-core heterogeneity [3].

carbon atoms (hexagonally packed), often containing vacancy – cluster defects as shown in Fig. 2. Butler and Diefendorf [5] have reported the skin to be between 100 and 150 nm thick. Wicks and Coyle [6], however, have reported the skin thickness to be in excess of 1  $\mu\text{m}$ . The core of the fibre is comprised of amorphous carbon arranged in a ribbon-like structure.

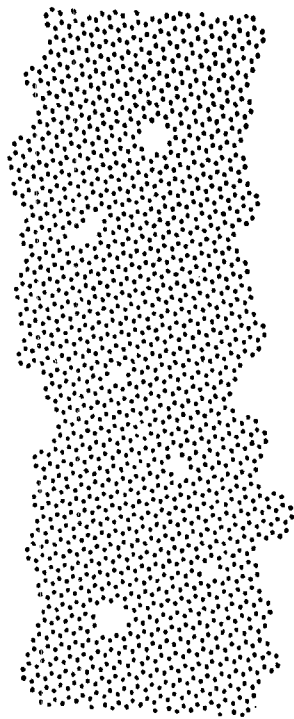


Figure 2 Structure of graphene showing vacancy-cluster defects [4].

Fig. 3 shows an end-on view of the fibres used in this investigation. The onion-skin structure of the fibre is evident. The X-ray diffraction pattern of the fibres showed one broad peak occurring at a value of  $2\theta$  for that of (0002) hexagonal graphite. The width of the peak indicates that the entire fibre is not crystalline, but that only a small fraction of the total material has this orientation. Based on Fig. 1, which schematically shows the skin-core heterogeneity present in ex-PAN fibres, and the information already published on the structure of these fibres, it is reasonable to assert that the onion skin of the fibres has an (0002) texture.

## 2.2. Composite materials

All of the composite samples used in this investigation consisted of Fortafil ex-PAN-based fibres and a glass matrix of a lithium aluminosilicate glass developed by Corning Glass (CGW 1723). The nominal composition of this glass is provided in Table II. Slight modifications were made to the glass due to the availability of chemicals; however, after melting, the composition was essentially 1723.

The method used to manufacture these composites has been described in great detail elsewhere [1, 7]; it will be mentioned here only briefly. The tape of fibres was cut to 10 cm lengths (approximately 4 in), and was suspended on a frame which gripped the fibre tows at both ends. A slurry consisting of glass powder, distilled water, an organic binder, and an organic surfactant was then poured over each side of the fibres. The infiltrated fibres were allowed to dry, and were then removed from the frame. Examination of the as-infiltrated plies on the scanning electron microscope (SEM) showed that the glass particles had penetrated completely through the fibre tows. Once enough plies were infiltrated, the plies were hot pressed at a temper-

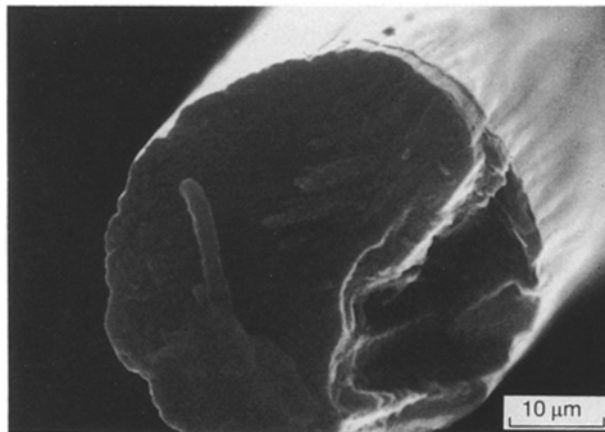


Figure 3 Scanning electron micrograph showing end-on view of a carbon fibre.

TABLE II Nominal composition of CGW 1723 (wt %)

Code	SiO <sub>2</sub>	B <sub>2</sub> O <sub>3</sub>	MgO	CaO	BaO	Al <sub>2</sub> O <sub>3</sub>
1723	57	4	7	9	7	16

ature of 1250 °C and a pressure of 6.9 MPa ( $10^3$  p.s.i.) for approximately 15 min. All the composites had a unidirectional lay-up consisting of seven infiltrated tapes. The final hot-pressed material had the dimensions 76 mm  $\times$  76 mm  $\times$  1.6 mm (3 in  $\times$  3 in  $\times$  0.065 in).

Using an application of Archimedes' principle, the unidirectional composites were found to have a fibre volume fraction of 0.49. This value was verified using quantitative metallographic techniques. Additionally, because of differences in coefficients of thermal expansion between the fibres and the glass matrix, the glass invariably cracked upon cooling from the hot-pressing temperature. Using quantitative metallographic methods, the composite material was found to have a volume fraction of microcracks of 0.6%  $\pm$  0.4%.

## 3. Experimental procedure

### 3.1. Carbon fibres

Carbon fibres were cut into initial lengths of 50 mm and placed in a vitreous silica holder. The holder and the fibres were then placed in an alumina boat, which was in turn pushed into the centre of an oxidation furnace. The tube of the furnace was made of quartz to minimize contamination. The oxidizing atmosphere was transported via a stainless steel gas delivery system. The gas flow rate was controlled with manual flow metres and was  $5.5 \times 10^{-7}$  m<sup>3</sup> s<sup>-1</sup> (33 cm<sup>3</sup> min<sup>-1</sup>).

Prior to an oxidation run, the furnace tube, alumina boat, and silica sample holder were baked at 800 °C for 3 h to remove adsorbed water vapour and any other volatile substances. The furnace set point was then lowered to the desired test temperature. After placing the sample in the furnace for a given period of time, both the sample holder and the fibres were removed from the furnace, placed in a desiccator to cool for 5 min, weighed, and replaced in the furnace.

All oxidation experiments were performed at 600 °C in 1.0, 0.21, and 0.05 atm (vol %) of oxygen.

### 3.2. Composite materials

The method used in oxidizing the composite samples made from carbon fibres and a matrix of 1723 glass is very similar to that used for the as-received fibres. Using a high-speed diamond saw, samples were cut having the following approximate dimensions: 13 mm × 13 mm × 1.6 mm (0.5 in × 0.5 in × 0.065 in). After cutting, the samples were ultrasonically de-greased and dried in a low-temperature oven. The samples were then oxidized using the same method as described in the preceding section.

## 4. Results

Fig. 4 shows the results obtained from the oxidation of the carbon fibres. The data are plotted as specific mass loss ( $\Delta\text{mass}/\text{initial surface area}$ ) versus time, as a function of oxygen partial pressure. The initial surface area was calculated knowing the initial length and diameter (50 mm and 7  $\mu\text{m}$ , respectively), the initial mass, and the density of the fibres. It was assumed that the entire surface area of the fibre participates in the oxidation reaction.

For all three oxygen partial pressures examined, a linear least-squares line provides the best functional relationship between specific mass loss and time. The slopes of these three lines are directly proportional to the oxidation rate of the fibres in the given partial pressure of oxygen. Assuming the rate of reaction is directly proportional to the surface coverage of oxygen on the exterior of the fibres, insight can be obtained into the nature of the fibres' surface.

If reaction rate versus  $\ln p$  is plotted, a linear relationship is obtained as shown in Fig. 5. This indicates that the oxidation of the carbon fibres exhibits Temkin - type adsorption kinetics. The significance of this will be discussed in a later section.

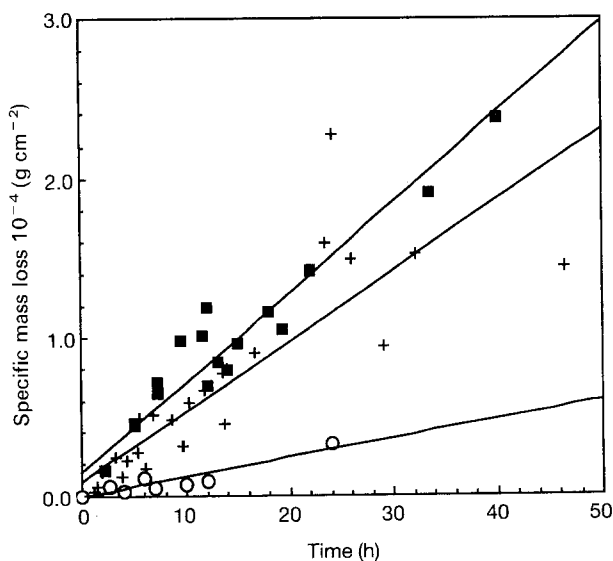


Figure 4 Oxidation data expressed as specific mass loss ( $\Delta\text{mass}/\text{initial surface area}$ ) versus time for carbon fibres as a function of oxygen partial pressure: (■) 100%  $\text{O}_2$ , (+) 21%  $\text{O}_2$ , (○) 5%  $\text{O}_2$ .

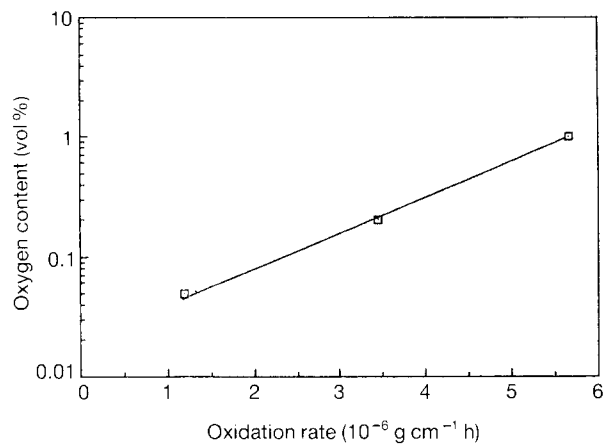


Figure 5 Plot of reaction rate versus  $\ln$  (oxygen partial pressure) showing Temkin-type adsorption kinetics for carbon fibres.

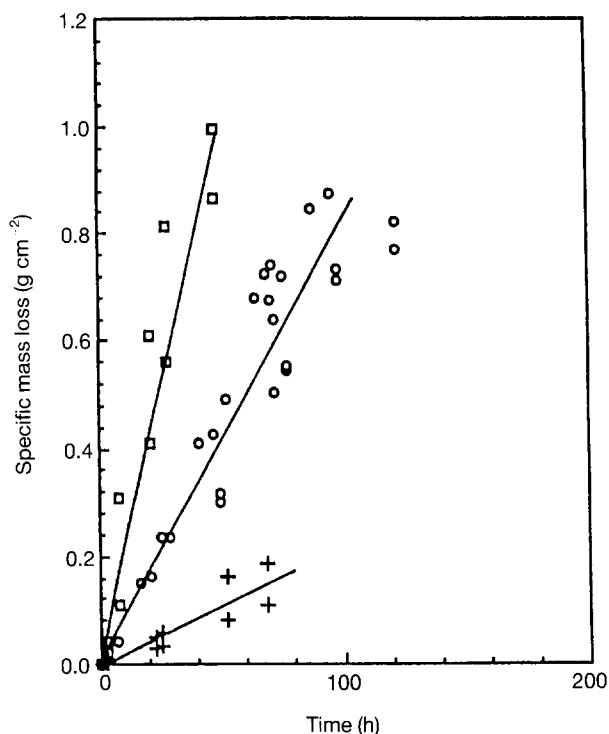


Figure 6 Oxidation data expressed as specific mass loss ( $\Delta\text{mass}/\text{initial surface area}$ ) versus time for a carbon fibre/glass matrix composite: (□) 100%  $\text{O}_2$ , (○) 21%  $\text{O}_2$ , (+) 5%  $\text{O}_2$ .

Fig. 6 shows the results obtained from the oxidation of the glass matrix/carbon fibre composite. Again, the data are plotted as specific mass loss ( $\Delta\text{mass}/\text{initial surface area}$ ) versus time. As only the ends of the fibres are initially exposed, this was the only surface area included in the normalization. Knowing the volume fraction of fibres in the composite, the mass and density of the composite, and the density and dimensions of the fibres, the number of fibres were calculated (per sample). The total surface area was then assumed to be  $2\pi r_0^2 N$ , where  $r_0$  is the initial radius of the fibres (7  $\mu\text{m}$ ) and  $N$  is the number of fibres. A linear least-squares fit best describes the data.

If the slopes of these three lines are plotted, i.e. the rate of reaction, versus oxygen partial pressure, a linear relationship is obtained as shown in Fig. 7. This is indicative of Langmuir-type kinetics, rather than the Temkin relationship obtained with the as-received

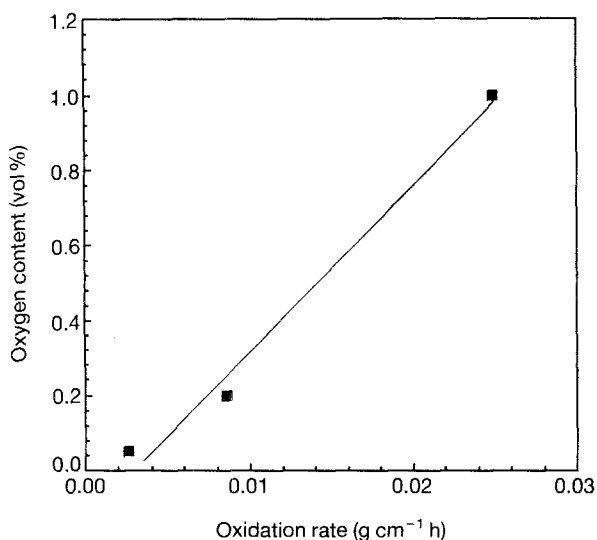


Figure 7 Plot of reaction rate versus oxygen partial pressure showing Langmuir-type oxidation for a carbon fibre/glass matrix composite.

fibres. This difference in oxidation kinetics is created by the highly anisotropic structure of the fibres, and will be discussed in a following section.

## 5. Discussion

### 5.1. The nature of surface reactions

To obtain a more thorough understanding of the oxidation of carbon fibres and the various factors that influence the process, such as oxygen partial pressure and catalysts, it is necessary to examine the ideas involved with surface-related processes such as adsorption. Many theories have been proposed to explain the nature of surface adsorption; however, only three will be discussed at this time: the Langmuir adsorption isotherm, the Freundlich adsorption isotherm, and the Temkin adsorption isotherm. All three isotherms predict the functional dependence of fractional equilibrium surface coverage,  $\theta$ , as a function of pressure of the adsorbed gas, where fractional surface coverage is defined as the number of occupied surface reaction sites divided by the total number of available surface reaction sites. If the rate of chemical reaction is a function of the fractional surface coverage, then these three isotherms yield the functional relationship between the rate of reaction and the partial pressure of the reactant gas, assuming the surface is in equilibrium. Because this assumption is reasonable, such comparisons can be made. First, the underlying principles of each isotherm should be understood.

The Langmuir adsorption isotherm is based on four important underlying assumptions.

1. Adsorption is localized and takes place only through the collision of gaseous molecules with vacant surface sites.
2. Each site can accommodate only one adsorbed molecule.
3. There is no interaction between adsorbed molecules.
4. All sites are energetically equal.

With these four assumptions, the Langmuir isotherm for non-dissociative adsorption yields the following

relationship between surface coverage and the partial pressure of the adsorbed species

$$\theta = \frac{aP}{1 + aP} \quad (1)$$

where  $P$  is the partial pressure of the adsorbed species in the surrounding atmosphere, and  $a$  is a constant. To determine if a surface reaction is exhibiting Langmuir-type adsorption kinetics, a plot of  $P/\theta$  versus  $P$  should produce a straight line [8].

When it became clear that not all surface reactions for every chemical system could be described by the Langmuir isotherm, Freundlich proposed the following relationship between surface coverage and partial pressure of the adsorbing species

$$\theta = (a_0 P)^{RT/q} \quad (2)$$

where  $a_0$  is a constant,  $R$  is the ideal gas constant,  $T$  the absolute temperature, and  $q$  the activation energy for the adsorption of one monolayer. Data which exhibit Freundlich-type adsorption kinetics will be linear on a plot of  $\log \theta$  versus  $\log P$ . Rideal [9] has shown that the Freundlich isotherm can be derived from the Gibbs adsorption equation. Kinetic derivations of the isotherm have been developed by Zeldovich [10], Halsey [11], and Halsey and Taylor [12].

The Temkin adsorption isotherm was derived with different initial conditions than the Langmuir isotherm. Temkin assumed that: (1) adsorption does not occur uniformly on a surface; (2) certain sites are more energetically favourable for adsorption, and these sites will be preferentially occupied; (3) the heat of adsorption decreases (becomes less negative) with increasing surface coverage. Based on these three statements, the following expression was derived for equilibrium fractional surface coverage

$$\theta = \frac{RT}{q_0 a} \ln(A_0 P) \quad (3)$$

where  $R$ ,  $T$ , and  $P$  have been previously defined;  $A_0$  and  $a$  are constants; and  $q_0$  is the heat of adsorption at  $\theta = 0$ . Data that exhibit Temkin-type adsorption kinetics will be linear on a plot of  $\theta$  versus  $\ln P$ .

The equations presented for the three adsorption isotherms are shown in their most elemental form. If the boundary conditions are changed in the original derivations, the original equations may be slightly altered. The functional dependence between  $\theta$  and  $P$ , however, will remain constant.

### 5.2. Carbon fibres

In Fig. 6, the reaction rates of the as-received fibres obtained in the various partial pressures of oxygen seem to exhibit Temkin-type adsorption kinetics. To apply Temkin adsorption kinetics to this system, it must be assumed that the surface coverage of oxygen on the fibres is in equilibrium, i.e. surface coverage is constant with time. Work by Walker *et al.* [13] supports the assertion that at 600 °C, the surface of the carbon fibres is in adsorptive equilibrium.

By exhibiting Temkin-type adsorption kinetics, a direct link can be made between the oxidation behavi-

our and the actual structure of the fibres. One of the underlying boundary conditions of the Temkin isotherm is that the adsorbing surface is not energetically uniform. In the bare fibres, the majority of available surface area is provided by the sides of the fibres, which consist of graphene. This graphene skin contains defects and vacancy clusters, which are very probably preferential sites for the adsorption of oxygen [14]. It is reasonable to assert that these defect sites are not energetically homogeneous, but rather exhibit a distribution of energies. The lowest energy sites will be occupied first, with the remaining locations being filled sequentially from lowest to highest energy configuration.

### 5.3. Glass matrix/carbon fibre composite

By varying the partial of pressure of oxygen in the ambient test environment, a linear relationship between specific mass loss and time is obtained at 600 °C. However, unlike the unprotected carbon fibres, the fibres in 1723 composites do not exhibit Temkin-type reaction kinetics. Plotting the oxidation rate versus  $\log(\text{pressure})$  does not produce a straight line. Only by plotting oxidation rate versus oxygen partial pressure is a linear relationship obtained, as is shown in Fig. 7. The data shown in Fig. 7 are of the form  $\theta = kP$ , where  $k$  is a constant, and  $\theta$  and  $P$  have been defined previously. This is the functional form for the Langmuir isotherm where the adsorption coefficient is small. (The adsorption coefficient is defined as the ratio of the adsorption rate constant to the desorption rate constant [15].) Because the relationship is linear with pressure, not with  $(\text{pressure})^{1/2}$ , the adsorbing species could be molecular oxygen. If this is true, there must be a step in the adsorption process in which molecular oxygen becomes atomic oxygen. This would imply that the system may not be in adsorptive equilibrium [16]. Experiments utilizing sophisticated high-vacuum techniques would have to be employed to obtain such specific information.

This difference between the oxygen partial pressure dependence of the weight loss data of the bare fibres and the fibres contained in the glass matrix composites can be explained by examining the structure of

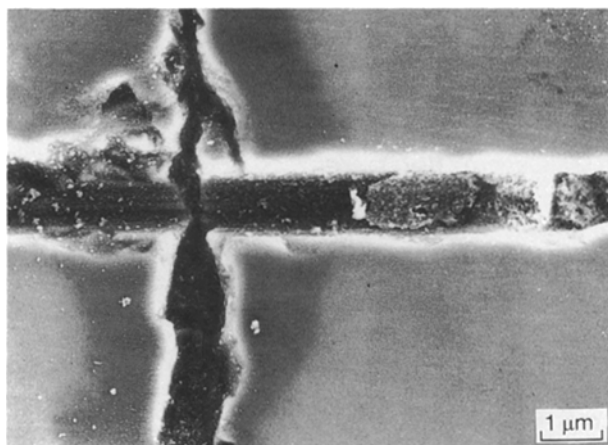


Figure 8 Scanning electron micrograph of a fibre/matrix interface in an oxidized composite sample.

the carbon surface that is exposed in each instance. In a 5 cm long fibre tow, most of the available surface area is generated by the sides of the cylindrical fibres. The structure of this surface is graphene with a (0002) texture, which is an energetically non-uniform surface.

The available fibre surface area in the composites, however, is a combination of the surface area of the exposed fibre ends, and the surface area created by fibre/microcrack intersections [1]. In the latter case, however, once the fibre skin has been consumed, the amorphous core is exposed, which has the same structure as a fibre end. The oxidation front advances perpendicular to the fibre axis, with the glass/fibre interface remaining intact. Microstructural evidence of this is provided in Fig. 8. In the composite matrix, therefore, the surface being oxidized is amorphous carbon, not graphene. This surface is more energetically uniform than the sides of the fibres. Therefore, the oxidation kinetics are most accurately described by the Langmuir adsorption isotherm, which is different from the Temkin-type behaviour exhibited by the bare fibres.

## 6. Conclusions

The oxidation data presented in this investigation reveal that the dependence of oxidation rate upon oxygen partial pressure is affected by the nature of the reactive surface. For the as-received fibres, most of the available reactive surface area is graphene. The suitable sites for adsorption contained on the graphene have a distribution of energies, which creates an energetically non-uniform surface. Oxidation rate as a function of partial pressure is best described by the Temkin adsorption isotherm.

For the fibres contained in the composite material, amorphous carbon constitutes that active oxidation surface. Because of the greater abundance of defects, the surface is more energetically uniform, and the relationship between oxidation rate and oxygen partial pressure is most accurately described by the Langmuir adsorption isotherm.

## References

1. R. G. IACocca and D. J. DUQUETTE, *J. Mater. Sci.* **28** (1993) 4749.
2. *Idem, ibid.* **28** (1993) 1113.
3. D. J. JOHNSON, in "Chemistry and Physics of Carbon", Vol. 20, edited by P. A. Thrower, (Marcel Dekker, New York, 1987) p. 1.
4. A. FOURDUEX, R. PERET and W. RULAND, in "Proceedings of the International Conference on Carbon Fibers, their Composites, and Applications", Plastics and Polymer Conference Supplement (The Plastics Institute, London 1971) p. 57.
5. B. L. BUTLER and R. J. DIEFENDORF, in "Papers on the 9th Conference on Carbon", Boston, MA (American Carbon Society, University Park, PA, 1969) p. 45.
6. B. J. WICKS and R. A. COYLE, *J. Mater. Sci.* **11** (1976) 376.
7. R. G. IACocca, PhD dissertation, Rensselaer Polytechnic Institute, Troy, NY (1991).
8. D. O. HAYWARD and B. B. W. TRAPNELL, "Chemisorption" (Butterworths, London 1964) pp. 161–9.
9. E. K. RIDEAL, "Surface Chemistry" (Cambridge University Press, Cambridge, 1930).
10. J. ZELDOWITSCH, *J. Physiochim.* **1** (1934) 961.

11. G. HALSEY, *Adv. Catal.* **4** (1952) 259.
12. G. HALSEY and H. S. TAYLOR, *J. Chem. Phys.* **15** (1947) 624.
13. P. L. WALKER Jr, L. G. AUSTIN and J. J. TIETJEN, "Chemistry and Physics of Carbon", Vol. 1 (Marcel Dekker, New York, 1965) p. 327.
14. B. J. WICKS and R. A. COYLE, *J. Mater. Sci.* **11** (1976) 376.
15. W. J. MOORE, "Physical Chemistry", 4th Edn (Prentice Hall, New Jersey, 1972) p. 498.
16. J. B. HUDSON, Rensselaer Polytechnic Institute, private communication, August 1991.

*Received 2 March  
and accepted 16 August 1993*